JBIC Journal of Biological Inorganic Chemistry (2023) 28:139–152
https://doi.org/10.1007/s00775-022-01977-w

ORIGINAL PAPER

Tryptone-stabilized silver nanoparticles' potential to mitigate planktonic and biofilm growth forms of *Serratia marcescens*

Pooja Pandey[1] · Kimaya Meher[1] · Berness Falcao[1] · Manu Lopus[1] · V. L. Sirisha[1]

Received: 14 June 2022 / Accepted: 19 October 2022 / Published online: 9 December 2022

Abstract

Several microbial pathogens are capable of forming biofilms. These microbial communities pose a serious challenge to the healthcare sector as they are quite difficult to combat. Given the challenges associated with the antibiotic-based management of biofilms, the research focus has now been shifted towards finding alternate treatment strategies that can replace or complement the antibacterial properties of antibiotics. The field of nanotechnology offers several novel and revolutionary approaches to eradicate biofilm-forming microbes. In this study, we evaluated the antibacterial and antibiofilm efficacy of in-house synthesized, tryptone-stabilized silver nanoparticles (Ts-AgNPs) against the superbug *Serratia marcescens*. The nanoparticles were of spherical morphology with an average hydrodynamic diameter of 170 nm and considerable colloidal stability with a Zeta potential of -24 ± 6.15 mV. Ts-AgNPs showed strong antibacterial activities with a minimum inhibitory concentration (MIC_{50}) of 2.5 µg/mL and minimum bactericidal concentration (MBC) of 12.5 µg/mL against *S. marcescens*. The nanoparticles altered the cell surface hydrophobicity and inhibited biofilm formation. The Ts-AgNPs were also effective in distorting pre-existing biofilms by degrading the extracellular DNA (eDNA) component of the extracellular polymeric substance (EPS) layer. Furthermore, reduction in quorum-sensing (QS)-induced virulence factors produced by *S. marcescens* indicated that Ts-AgNPs attenuated the QS pathway. Together, these findings suggest that Ts-AgNPs are an important anti-planktonic and antibiofilm agent that can be explored for both the prevention and treatment of infections caused by *S. marcescens*.

✉ V. L. Sirisha
sirisha@cbs.ac.in

Pooja Pandey
pooja.pandey@cbs.ac.in

Kimaya Meher
kimaya.meher@cbs.ac.in

Berness Falcao
bernessfalcao@gmail.com

Manu Lopus
manu.lopus@cbs.ac.in

[1] School of Biological Sciences, UM-DAE Centre for Excellence in Basic Sciences, University of Mumbai, Kalina Campus, Santacruz East, Mumbai, India

Graphical abstract

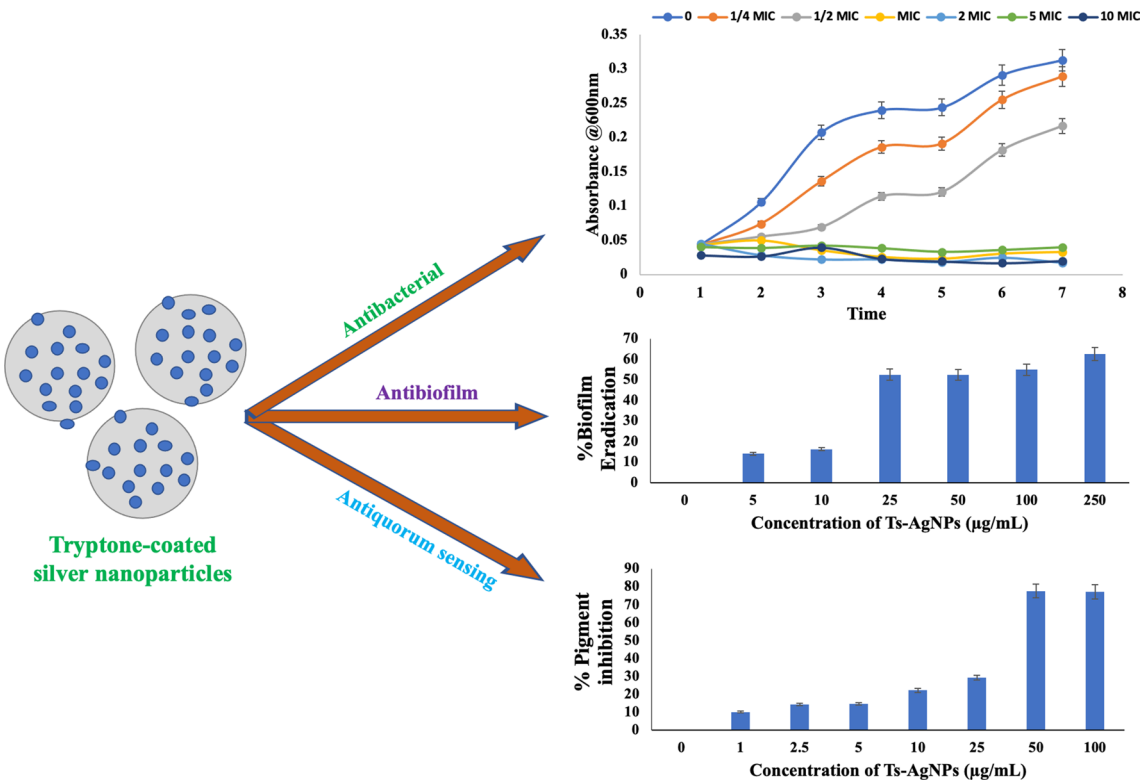

Keywords Silver nanoparticles · Antibacterial · Antibiofilm · Anti-quorum sensing · Tryptone

Introduction

Infections caused by antibiotic-resistant bacterial strains are a leading cause of mortality and have an overall detrimental effect on public health and the health economy worldwide [1]. One of the potential mechanisms of bacteria to attain antibiotic resistance is through biofilm formation. By definition, a biofilm is formed by bacterial colonies with the potential to collectively grow and adhere to biotic or abiotic surfaces into a 3-dimensional network [2]. This complex 3D multi-layered network holds resting bacteria, which have the potential to move on another surface, leading to the formation of a new biofilm on maturing. The extracellular protective layer of biofilms is composed of various proteins, nucleic acids, and other biomolecules. These biomolecules' network with entrenched cells in the biofilm helps in adherence and protection from harsh environments and bactericides. They also play a key role in the manufacturing of metabolites and nutrition for the bacteria [3, 4]. Biofilms play an important role in shielding bacterial strains against antibiotics. This is achieved by slowing down the process of antibiotic penetration, enzymatically degrading the antibiotics, and supporting bacterial cells to develop resistance at the gene level. Targeting these biofilms can render bacterial cells vulnerable to antibiotics and are a great target for antimicrobial therapy [4, 5]. Laboratories across the world have been exploring different therapeutic strategies including bacteriophage therapy, antimicrobial peptides, surface modulators, natural compounds, and metallic nanoparticles for controlling these bacterial biofilms [6–9].

Among these, the definitive advantage of using metallic nanoparticles is that they display a wide range of physicochemical properties, compared to their bulk analogues and are easily tuneable. Nanoparticles of the size between 1 nm to 200 nm exert unique and novel properties in biological systems [10–14]. These properties are attributed to their high surface energy, minimal imperfections, large proportion of surface atoms, and spatial confinement. Silver has been known to possess strong antimicrobial properties since ancient times [15, 16]. It has been in use for preventing and treating microbial infections for more than 5 millennia. In recent times, silver is also known to prevent viral infections [17]. It is also used in the form of silver-impregnated polymer on medical devices

and implants used for surgery. With the advent of nanotechnology, silver nanoparticles (AgNPs) have been investigated extensively in several biomedical applications. Several 'green synthesis' approaches utilizing the reducing power of plant polyphenols, peptides, microbes, etc. have been explored with varying degrees and definitions of success [18]. Specifically, proteins and other chemicals present in these biomaterials act as reducing-capping or stabilizing agents during the synthesis process [19, 20]. These biological methods for metallic nanoparticle synthesis have gained credence and momentum over the past decade [21].

For the current study, we made use of tryptone (trypsinized casein) as the stabilizing agent for the silver nanoparticles. Tryptone, by itself, has no toxicity to bacteria. On the contrary, it is a vital component in several nutrient media used to grow bacteria [22, 23]. Nevertheless, it is an excellent stabilizing agent. As we have reported earlier, both gold and silver nanoparticles that are stabilized with tryptone have considerable anticancer potential [11–14]. Given that tryptone by itself has no considerable antibacterial effect, it can be used for surface functionalization of silver. This method would enable pinpointing of the stand-alone mechanism of action of nanosilver in bacterial cells, without the considerable contribution from the stabilizing agents.

In the current study, silver nanoparticles stabilized with tryptone (Ts-AgNPs) were tested for their antibacterial and antibiofilm potential against respiratory tract infection-causing bacteria *S. marcescens*.

Materials and methods

Synthesis and characterization of silver nanoparticles

Ts-AgNPs were synthesized and characterized as we have reported earlier [14]. Briefly, 1 mg/mL tryptone (pH 12) (SRL, Bangalore, India) was mixed with 1 mM of silver nitrate (SD fine chemicals, Mumbai, India) and the solution was kept for heating for 20 min in the dark till the colour changed to dark brown. The following day, the nanoparticles were collected by centrifugation (26,200×*g*) for 30 min and the pellets were dried using a Labconco FreeZone 2.5 lyophilizer. The formation of Ts-AgNPs was confirmed by observing the UV–Vis spectrum (Infinite® 200 PRO, Tecan, Switzerland). The core size and shape of the Ts-AgNPs were visualized using a transmission electron microscope. The hydrodynamic diameter and the stability of the synthesized Ts-AgNPs were checked using a Zetasizer Nano-ZS90 size analyser (Malvern Instruments Ltd, Worcestershire, UK). The Fourier-transform infrared (FTIR) spectral analysis was employed to detect the presence of different functional groups on the nanoparticles [14].

Minimum inhibitory concentration (MIC) and minimum bactericidal concentration (MBC) determination assay

To check the antibacterial potential of Ts-AgNPs against *S. marcescens*, minimum inhibitory concentration was assessed using the microdilution method as mentioned in Clinical and Laboratory Standards Institute [23] guidelines followed by MTT (3-(4,5-Dimethylthiazol-2-yl)-2,5-Diphenyltetrazolium Bromide) assay. Briefly, 10^6 CFU/mL bacterial cells were suspended in microtiter plates containing serially diluted Ts-AgNPs (1−10 µg/mL). The plates were incubated at 37 °C for 24 h and bacterial cell viability was determined using MTT as mentioned in Vishwakarma and Vavilala 2020. To check if Ts-AgNPs have a bactericidal effect on *S. marcescens*, minimum bactericidal activity was then determined. For this 24 h, Ts-AgNPs treated bacterial cells were taken, Ts-AgNPs were removed, and the bacterial cells were supplied with fresh medium and allowed to grow for another 24 h. After incubation, viable cells were determined by staining with MTT assay as mentioned above [24].

Time–kill curves and colony-forming unit (CFU) assay

To check the potential of Ts-AgNPs to inhibit bacterial growth over time, a time–kill curve was performed. For this experiment, 10^6 CFU/mL cells were treated with different concentrations of Ts-AgNPs (0–10 MIC) and bacterial growth was monitored from 0 h till 48 h by taking the optical density @595 nm using a spectrometer. Then, growth–kill curves were plotted by plotting the optical density vs time [25].

Colony forming unit assay was performed, by taking 10^6 CFU/mL culture treated with different concentrations of Ts-AgNPs and incubated for 37 °C for 24 h. Post-incubation, 100 µL of this culture was spread on fresh GM3 medium and incubated further 24 h at 37 °C. Post-incubation, the number of colonies formed were counted manually and compared with untreated control [25].

Intracellular reactive oxygen species (ROS) determination

To check if Ts-AgNPs induce endogenous reactive oxygen species production, this assay was performed. For this experiment, overnight grown culture was further inoculated in fresh GM3 medium and incubated at 37 °C for 3–4 h until the O.D. of the culture reaches to 0.5. Then, 100 µL of this culture was suspended in 96-well microtiter plates, and then, 100 µM 2′,7′-dichlorodihydrofluorescein

diacetate (DCFDA) was added. Further, different concentrations of Ts-AgNPs (0–5 MIC) were added into these wells, mixed well, and kept in dark for 3 h and 5 h. The amount of ROS produced was monitored by measuring the fluorescence of highly fluorescent dichlorofluorescein (DCF) formation in presence of ROS by exciting at 485 nm and emission at 535 nm using Tecan UV–Vis spectrophotometer [26, 27].

Hydrogen peroxide sensitivity assay

To validate the antibacterial ability of Ts-AgNPs by inducing ROS, this assay was performed. Briefly, 10^6 CFU/mL overnight culture was further inoculated in fresh medium and different concentrations of Ts-AgNPs (0-5MIC) were added and incubated further 24 h at 37 °C. Post-incubation, 100 µL of this culture was spread on GM3 agar plate. A sterile 6 mm Whatman paper disk was placed in the middle of the plate and 10 µL of 3% hydrogen peroxide was added to the paper disc placed at the centre. These plates were incubated at 37 °C for 24 h. After incubation, the zone of inhibition was measured. The experiment was repeated thrice for each concentration of the Ts-AgNPs and untreated controls [28].

Biofilm Inhibition studies

The property of silver nanoparticles to inhibit the formation of biofilms was assessed using biofilm inhibition assay. Bacterial culture (overnight grown) was sub-cultured in fresh GM3 media and allowed to grow until an O.D. reaches to 0.5. This culture was further treated with different concentrations of Ts-AgNPs (0–100 µg/mL) and incubated for 24 h, 37 °C, 120 rpm. The planktonic cells and unadhered cells were removed, washed three times using distilled water, and dried for 10 min at room temperature. After drying, 200 µL of 1% crystal violet stain was added to each well and placed at room temperature for 30 min. The excess stain was washed off and 200 µL of ethanol (100%) was added to all wells. The O.D. was measured using a spectrophotometer at 595 nm [29].

Cell-surface-hydrophobicity assay

The effect of Ts-AgNPs on the hydrophobicity of bacterial cells to inhibit biofilm formation was evaluated using the Bacterial Adherence to Hydrocarbon (BATH) Assay. A 10^6 CFU/mL cells were incubated with different concentrations of Ts-AgNPs (0–100 µg/mL) for 24 h at 37 °C, 120 rpm. After incubation, absorbance values were obtained at 600 nm. The reaction mixture was then transferred to glass tubes with equal volumes of absolute toluene in each tube. After vigorous shaking for 30 sec, the tubes were incubated for 5 min at room temperature for phase separation. After separation, the aqueous layer was collected into a 96-well plate and the optical density was measured at 600 nm [25].

Biofilm eradication assay

This assay is carried out to examine the ability of Ts-AgNPs to eradicate or disintegrate preformed biofilms. Approximately 10^6 CFU/mL of cells were treated with 15 mM hydrogen peroxide and incubated for 24 h at 37 °C to form a biofilm. After 24 h of incubation, planktonic cells were removed slowly and fresh medium with varying concentrations of Ts-AgNPs was added to the wells and incubated for 24 h at 37 °C, 120 rpm. Further, unadhered cells were washed using distilled water and biofilms in the wells were quantified using the crystal violet assay as mentioned above. The assay was performed thrice, and percentage eradication was graphically represented against Ts-AgNPs' concentration [30, 31].

Quantification of extracellular polymeric substance (EPS)

Extracellular polysaccharide is the matrix that helps in the protection as well as maintains the structural and functional integrity of the biofilm. To examine the ability of Ts-AgNPs in distorting the EPS layer, this assay was performed. In this assay, preformed biofilms were treated with different concentrations of Ts-AgNPs and incubated at 37 °C for 24 h. After 24 h, equal volumes of absolute acetone and 10% trichloroacetic acid (TCA) were added to the EPS extract and incubated at 4 °C overnight. After incubation, the tubes were centrifuged at 8000 rpm for 5 min at 25 °C. The supernatant was gently discarded and the pellet was air dried. The weights of the pellets of both untreated and Ts-AgNPs-treated samples were measured and the results were represented as a graph of the total weight of EPS against the concentration of Ts-AgNPs [32].

eDNA quantification

Extracellular DNA (eDNA) isolation was performed using a modified protocol by Wang et al. [33]. Preformed biofilms in microtiter plates were treated with different concentrations of Ts-AgNPs and eDNA was extracted from the EPS layer by incubating the biofilms at 4 °C for 1 h, after which 1 µL of 0.5 M of EDTA was added to each well. The contents of wells were carefully transferred into the microfuge tubes and centrifuged. The pellet was resuspended into 50 mM Tris HCL (pH 8). eDNA was then isolated by adding an equal volume of phenol:chloroform:isoamyl alcohol (25:24:21 and

centrifuged for 5 min at 10,000 rpm. To the aqueous layer, three equal volumes of ice-cold ethanol along with 1/10th amount of sodium acetate (pH 5.2) were added and stored overnight at − 20 °C. After incubation, tubes were centrifuged at 18,000*g*, 4 °C for 20 min. The pellet was allowed to dry and resuspended in Tris:EDTA buffer. The concentration and purity of the eDNA extracted were calculated spectrophotometrically by measuring the absorbance ratio A_{260}/A_{280} using nanoquant200©.

Fluorescent microscopy analysis

To validate the biofilm eradicating potential of Ts-AgNPs, fluorescence microscopy analysis was carried out. Biofilms were preformed on the coverslips and these pre-existing biofilms were then treated with ½ MIC and MIC of Ts-AgNPs for 24 h at 37 °C. Post-incubation, the biofilms were washed with phosphate buffer saline (PBS) twice. Then, the biofilms were stained with 10 µ/mL of propidium iodide and kept in the dark for 20 min. After staining, the coverslips were washed with Milli Q water and mounted on the slides. Slides were observed under fluorescent microscopy in TRITC filters at 100 X with oil immersion [34].

Analysis of quorum-sensing pathway-induced virulence factors

Quorum sensing pathway is known to induce various virulence factors in *S. marcescens* and contribute to its pathogenicity. To check the effect of Ts-AgNPs in inhibiting these virulence factors production, quantification of urease, protease, lipase, hemolysin, and prodigiosin pigment production was carried out.

Urease assay

For urease assay, overnight grown culture of Ts-AgNPs treated/untreated cells was centrifuged at 8499 × *g* at 25 °C for 5 min and 0.1 mL of supernatant was treated with 0.5 mL of 2% urea, incubated at 37 °C for 3 h. Post-incubation, the amount of ammonia released was quantified by adding 0.1 mL of Nessler's reagent and incubated for another 5 min at room temperature. Urease activity was quantified by measuring the O.D. at 530 nm using a UV–Visible spectrophotometer [35].

Protease assay

Azocasein assay was performed to determine the proteolytic action of *S. marcescens* in the presence/absence of Ts-AgNPs. For this experiment, 75 µL of Ts-AgNPs treated/untreated cell-free supernatant was reacted with 125 µL of azocasein substrate (0.3% azocasein in 0.05 M Tris–HCl + 0.5 mM $CaCl_2$). The mixture was then incubated for 15 min at 37 °C. The reaction was then stopped by adding 600 µL 10% trichloroacetic acid and incubated at − 20 °C for 20 min. The mixture was then centrifuged at 8000 rpm for 5 min. Then, 700 µL of NaOH was added to the supernatant and the protease activity was measured at 534 nm [36].

Hemolysin assay

Ts-AgNPs treated and untreated bacterial cultures were centrifuged at 11,000 rpm for 20 min at 4 °C. Then, 900 µL of fresh sheep blood suspension (2% sheep blood erythrocytes in PBS; pH 7.4) was added to 100 µL of supernatant. The mixture was incubated at 37 °C for 1 h. Then, the suspension was centrifuged at 3000 rpm for 10 min and the amount of hemoglobin released in the supernatant was measured at 530 nm. Erythrocytes suspended in distilled water served as positive control and erythrocytes suspended in PBS served as a negative control for this experiment [37]. Hemolysin activity was determined using the formula below:

$$\text{Percentage lysis} = \left[(\text{A530 of sample} - \text{A530 of background}) / (\text{A530 of total} - \text{A530 of background})\right] * 100.$$

Lipase assay

Overnight grown Ts-AgNPs treated and untreated bacterial cultures were centrifuged at 10,000 × *g* for 10 min at 4 °C. Pellet was dissolved in 0.5 mL of Tris–EDTA buffer (pH 8.0), and the resultant suspension was sonicated to release lipase from the cells. After sonication, the suspension was centrifuged, and the supernatant was collected to check lipase activity. To 0.1 mL of cell-free supernatant, 0.9 mL of *p*-nitrophenyl palmitate (pNPP) substrate mixture (solution A- 3 mg of pNPP in 1 mL isopropanol and solution B- 10 mg of gum arabic and 40 mg of Triton-X in 9 mL of 50 mM Tris–HCl buffer pH 8) was added, and incubated for 20 min at 60 °C in a shaking water bath. The lipase activity was measured spectrophotometrically at 400 nm [38].

Prodigiosin pigment production

Overnight grown culture was further inoculated in fresh GM3 medium, treated with different concentrations of Ts-AgNPs, and incubated for 24 h at 37 °C. The cells were then harvested at 10,000 rpm for 10 min. Prodigiosin pigment from *S. marcescens* cell pellet was extracted using 1 mL of acidified ethanol. The extracted pigment was quantified at 535 nm using UV–visible spectrophotometer [36].

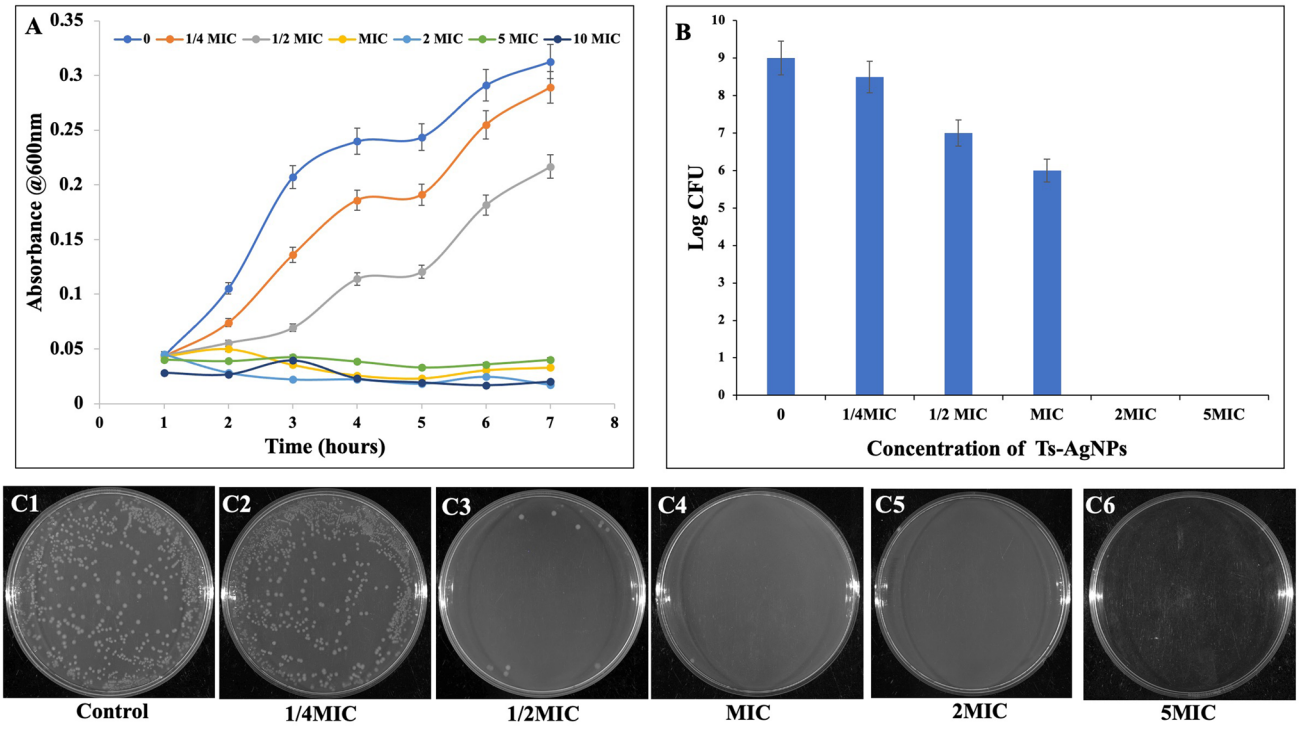

Fig. 1 Antibacterial potential of Ts-AgNPs against *S. marcescens*. **A** Time–kill curves. **B** CFU assay (C1–C6). Representative images of *S. marcescens's* ability to form colonies in the presence/absence of Ts-AgNPs. Data are the means of three independent experiments ± SE. ($p < 0.05$)

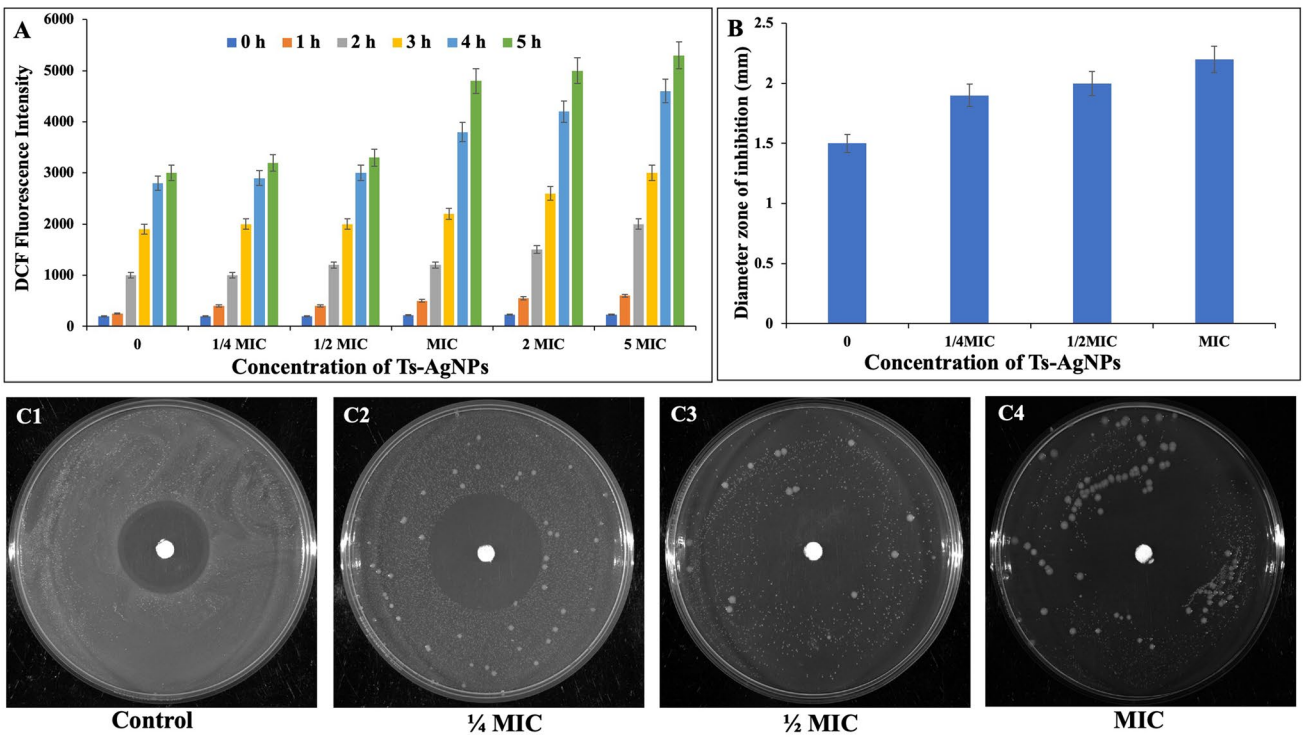

Fig. 2 Ts-AgNPs potential to induce reactive oxygen species in *S. marcescens*. **A** Quantification of intracellular ROS and **B** H_2O_2 sensitivity assay (**C1**–**C4**). Data are the means of three independent experiments ± SE. ($p < 0.05$)

Effect of Ts-AgNPs on swimming and swarming motilities of *S. marcescens*

The effects of Ts-AgNPs on *S. marcescens* swimming and swarming motilities were assayed. For this experiment, GM3 media with 0.3% and 0.5% agar plates without and with Ts-AgNPs (1/8 MIC, ¼ MIC, and ½ MIC) were prepared and 5 µL of *S. marcescens* culture was placed at the centre of the plate and incubated at 37 °C for 24 h in a plate incubator. After 24 h, the swimming and swarming motility of *S. marcescens* was measured in millimetres (mm) and reported in comparison to untreated controls [39].

Results

Synthesis and characterization of Ts-AgNPs

As we have reported [14], UV–Vis spectral analysis showed the maximum peak at 408 nm confirming the formation of the Ts-AgNPs. Transmission electron microscopy revealed ~ 18 nm core size and spherical morphology of the particles. The hydrodynamic diameter of the Ts-AgNPs was found to be ~ 170 nm and the zeta potential of -24 ± 6.15 mV confirmed the stability of the nanoparticles. The presence of different functional groups like amines, amides, aldehydes, and aromatic compounds indicated that tryptone played a crucial role in capping and stabilization of the Ts-AgNPs [14].

Antibacterial studies

The minimum inhibitory concentration (IC_{50}) of Ts-AgNPs against *S. marcescens* was found to be 2.5 µg/mL. Ts-AgNPs showed a bactericidal effect on *S. marcescens*, indicating that Ts-AgNPs were very effective in killing the bacteria and can help treat *S. marcescens*-associated infections.

Growth kill assay was performed to monitor the bacterial growth with respect to varying time points and concentrations of Ts-AgNPs. The graph obtained showed that there was a significant decrease in the number of viable cells of *S. marcescens* as the concentration of Ts-AgNPs increases (Fig. 1A). Ts-AgNPs significantly affected the log phase growth of this bacteria showing its bactericidal effect. Initially, the growth pattern was similar for all concentrations, but as the time increases, there was a gradual decrease in the number of viable cells. After 24 h, a steady growth pattern was seen in the untreated sample, whereas for treated samples, the number of viable cells decreased significantly with the increased concentration of Ts-AgNPs in a dose-dependent manner. A stark decrease in growth was observed from MIC till 10 MIC of Ts-AgNPs for *S. marcescens* (1A).

Moreover, it was observed that Ts-AgNPs significantly affected the colony-forming ability of *S. marcescens* cells. It was observed that when the cells were incubated with different concentrations of Ts-AgNPs, there was a significant decrease in the CFU in this bacterium (Fig. 1B). At $1/4^{th}$ and ½ MIC of Ts-AgNPs, there was a significant decrease in the number of bacterial colonies formed by *S. marcescens* as compared to the untreated control sample, whereas at MIC till 5 MIC of Ts-AgNPs treated bacteria showed no colonies (Fig. 1C). This indicates that Ts-AgNPs has a significant effect on colony-forming ability of *S. marcescens* in a concentration-dependent manner.

Intracellular ROS quantification

To explore the probable mechanism of Ts-AgNPs-induced bacterial death, intracellular ROS was quantified. It was observed that Ts-AgNPs inhibited bacterial growth by inducing ROS. Ts-AgNPs-treated bacteria showed a significant increase in ROS accumulation in a dose-dependent manner over time as compared to control. There was a maximum of ~ 2.5-fold increase in ROS production after 1 h Ts-AgNPs treatment. While at 3 h and 5 h, there was a maximum of 1.57- and 1.76-fold increase in ROS was observed in Ts-AgNPs-treated cells as compared to untreated control (Fig. 2A), indicating that Ts-AgNPs changing the redox environment in *S. marcescens* that led to bacterial cell death.

To substantiate the ability of Ts-AgNPs to induce ROS and kill bacteria, H_2O_2 sensitivity assay was performed. The results obtained clearly showed that with increased concentration of Ts-AgNPs, there was a gradual increase in the bacterial growth inhibition as indicated by increased diameter of the zone of inhibition (Fig. 2B). As compared to plain H_2O_2 disk, there was a 1.5-fold increase in the diameter of bacterial growth inhibition at MIC of Ts-AgNPs indicating the potential of Ts-AgNPs in inducing ROS and oxidative damage to *S. marcescens* (Fig. 2C1–C4).

Biofilm-inhibition assay

Ts-AgNPs-treated cells showed decreased biofilm formation as compared to control in a dose-dependent manner. It was observed that Ts-AgNPs showed 29–90% of inhibition of biofilm formation in *S. marcescens* at 1–100 µg/mL concentrations (Fig. 3A). This result indicates the potential of Ts-AgNPs to efficiently prevent the bacteria from adhering to the surface and initiate biofilm formation.

To determine the mechanism by which Ts-AgNPs inhibit biofilm formation, the cell surface hydrophobicity assay was performed. The graph obtained showed that with increased concentration of Ts-AgNPs, there was a gradual decrease

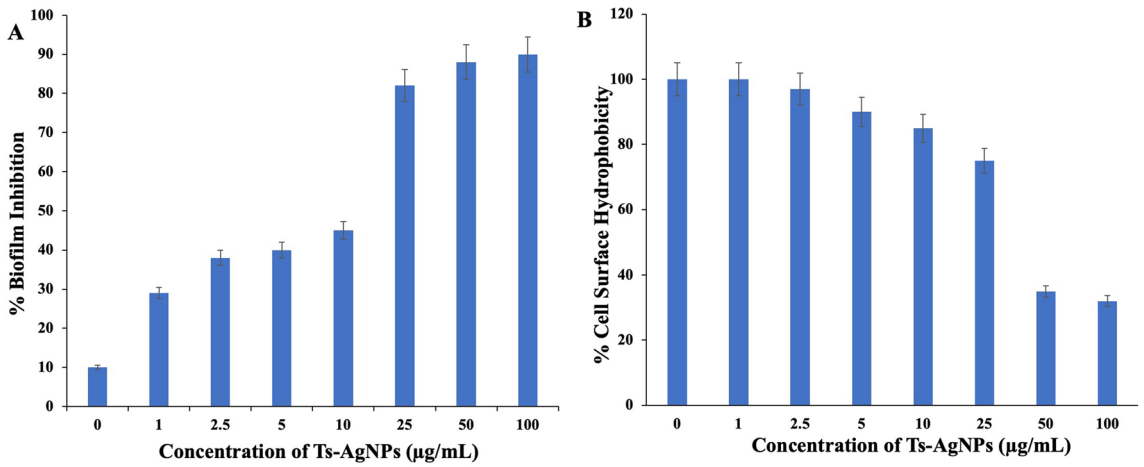

Fig. 3 Inhibition of biofilm formation by Ts-AgNPs in *S. marcescens*. **A** Biofilm-inhibition assay. **B** Cell-surface-hydrophobicity assay. Data are the means of three independent experiments ± SE. ($p < 0.05$)

in the hydrophobicity of the *S. marcescens* cells. Treated cells showed 15–70% reduced cell surface hydrophobicity at 1–100 µg/mL of Ts-AgNPs as compared to control (Fig. 3B). This indicates that Ts-AgNPs effectively altered the hydrophobic nature in this bacterium, which is a crucial determinant in the initial attachment of the cells to the substrate in the course of forming a biofilm. Therefore, Ts-AgNPs can be developed into a promising antibiofilm agent to prevent bacterial biofilms.

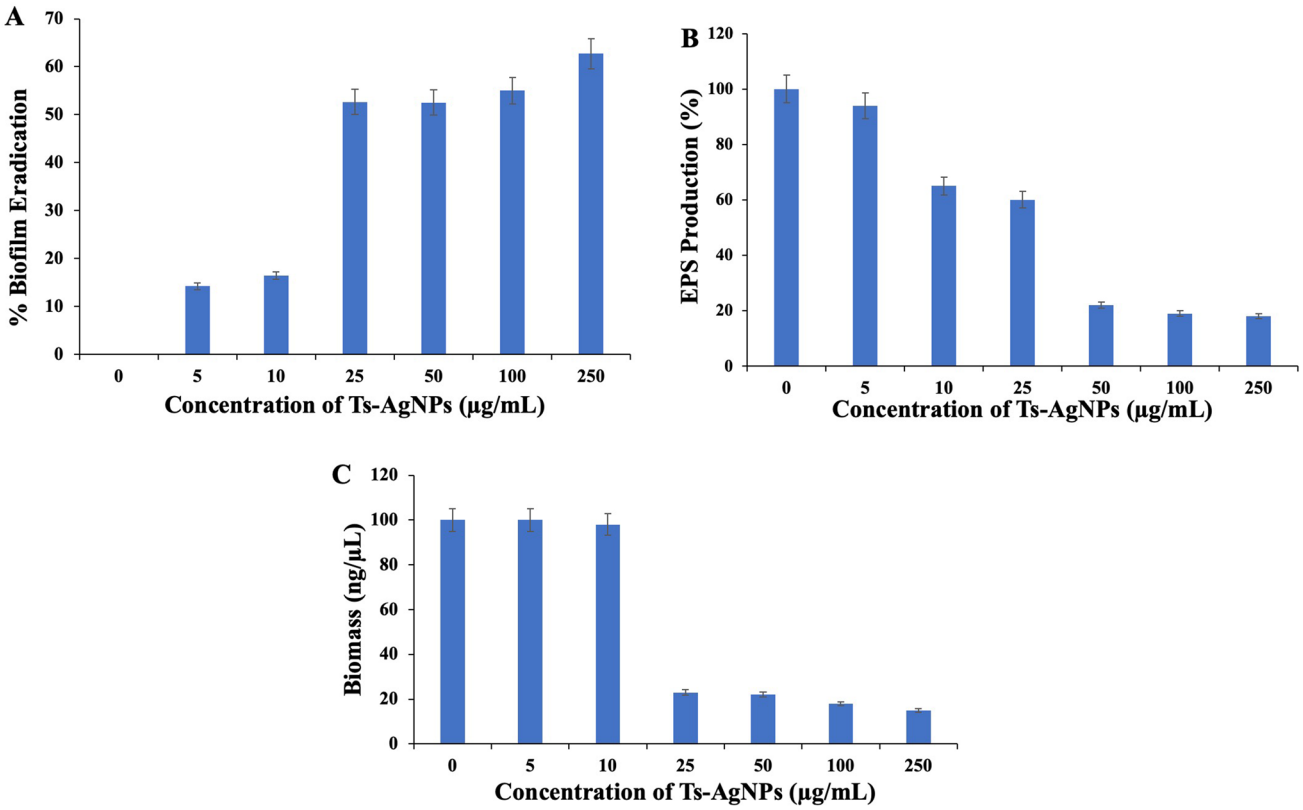

Fig. 4 Eradication of preformed biofilms of *S. marcescens* by Ts-AgNPs. **A** Biofilm eradication assay. **B** EPS quantification. **C** eDNA quantification. Data are the means of three independent experiments ± SE. ($p < 0.05$)

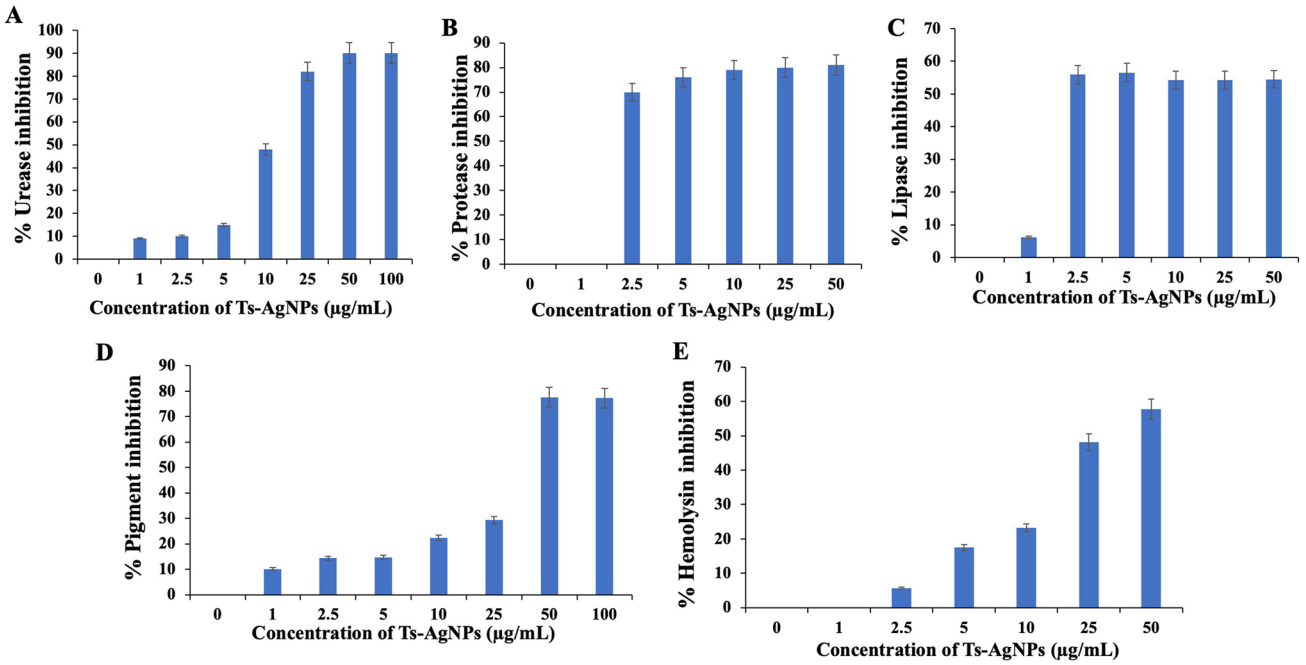

Fig. 5 Anti-quorum-sensing potential of Ts-AgNPs. **A** Urease assay, **B** protease assay, **C** lipase assay, **D** prodigiosin pigment production, and **E** hemolysin assay. Data are the means of three independent experiments ± SE. ($p < 0.05$)

Biofilm eradication assay

Eradication of preformed biofilm by Ts-AgNPs was determined by performing this assay. The results showed that *S. marcescens* preformed biofilms were effectively distorted with increased concentration of Ts-AgNPs. Bacteria treated with 5–25 µg/mL of Ts-AgNPs showed 14%, 17%, and 53% distortion of biofilms, respectively. While, 53%, 55%, and 63% distortion were observed at 50 µg/mL, 100 µg/mL, and 250 µg/mL of Ts-AgNPs-treated cells as compared to control (Fig. 4A).

To determine the ability of Ts-AgNPs in distorting this outer protective covering, quantification of EPS content was performed. It was observed that after centrifugation, the pellet of Ts-AgNPs-treated samples gradually decreased in a dose-dependent manner in comparison to the untreated sample. There was approximately 78% and 82% decrease in the weight of pellets at 50 µg/mL and 250 µg/mL of Ts-AgNPs, respectively, as compared to the control samples (Fig. 4B). This confirms the ability of Ts-AgNPs in disrupting the EPS layer of preformed biofilms in *S. marcescens.*

In the aim to determine the mechanism by which Ts-AgNPs distort the EPS covering in *S. marcescens*, quantification of eDNA of the EPS layer was carried out in both Ts-AgNPs treated and untreated samples. It was observed that the amount of eDNA isolated from the cell-free supernatants of Ts-AgNPs-treated samples of *S. marcescens* gradually decreased as compared to the untreated sample. Ts-AgNPs-treated cells showed a 4.3-fold decrease in the eDNA content of the EPS layer at 25 µg/mL. A maximum of 6.6-fold decrease in eDNA was observed at 250 µg/mL concentration of Ts-AgNPs, indicating their potential in degrading the eDNA component of the EPS layer and dissolving the biofilms (Fig. 4C).

Microscopy analysis

The ability of Ts-AgNPs in distorting preformed biofilms is further validated by fluorescence microscopy analysis. Preformed biofilms were stained with propidium iodide, showed densely packed aggregates of bacterial cells with intense fluorescence (Suppl Fig. 1A). While, the ½MIC, MIC, and 2 MIC Ts-AgNPs-treated preformed biofilms showed distorted biofilms with loosely packed small clusters of bacteria (Suppl Fig. 1B–D) validating the effect of Ts-AgNPs in eradicating matured biofilms.

Anti-quorum-sensing studies: quantification of virulence factors

It was observed that Ts-AgNPs significantly reduced QS-induced virulence factor production in *S. marcescens*. Urease activity was reduced to 48%, 82%, and 90% at 10 µg/mL, 25 µg/mL, and 100 µg/mL of Ts-AgNPs (Fig. 5A). ExoProtease activity was reduced to a maximum of 70–81% at 2.5–50 µg/mL concentration of Ts-AgNPs (Fig. 5B).

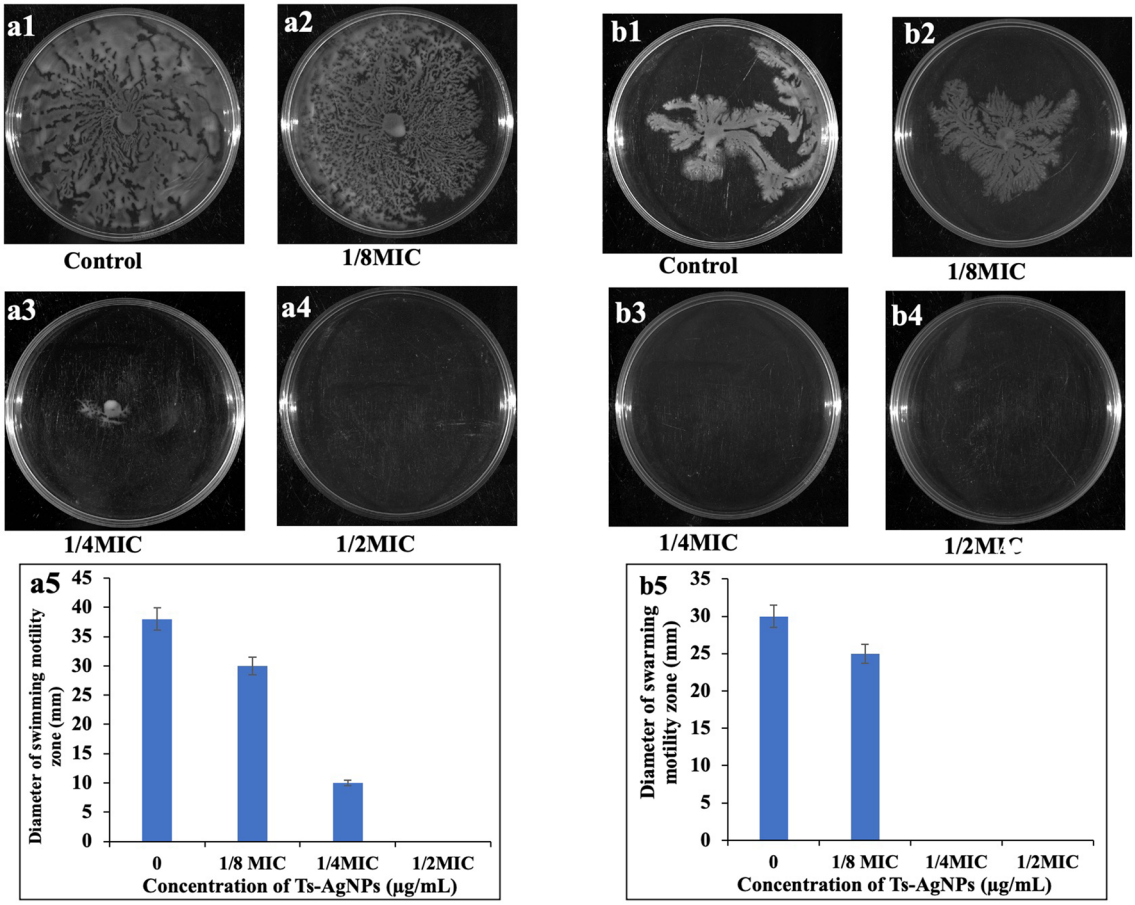

Fig. 6 **a** Swimming motility of *S. marcescens* in the absence/presence of Ts-AgNPs. **a1** Control, **a2** 1/8th MIC Ts-AgNPs, **a3** 1/4th MIC Ts-AgNPs, **a4** ½ MIC Ts-AgNPs, and **a5** diameter of swimming motility in presence of Ts-AgNPs. Data are the means of three independent experiments ± SE. ($p < 0.05$). **b** Swarming motility of *S. marcescens* in the absence/presence of Ts-AgNPs. **b1** Control, **b2** 1/8th MIC Ts-AgNPs, **b3** 1/4th MIC Ts-AgNPs, **b4** ½ MIC Ts-AgNPs, and **b5** diameter of swimming motility in presence of Ts-AgNPs. Data are the means of three independent experiments ± SE. ($p < 0.05$)

Similarly, lipase activity was significantly reduced with increased concentrations of Ts-AgNPs. It was observed that about 56% reduced lipase activity was observed from 2.5 to 50 µg/mL of Ts-AgNPs as compared to untreated control (Fig. 5C). Prodigiosin, an important pigment produced by *S. marcescens,* was significantly decreased to about 30–77% in 25–100 µg/mL of Ts-AgNPs-treated bacterial cells (Fig. 5D). Another important virulence factor produced by *S. marcescens* in hemolysin. Ts-AgNPs-treated cells showed ~ 20–60% reduced hemolysin production (Fig. 5E). These results indicate the promising potential of silver nanoparticles in attenuating the quorum-sensing pathway and its associated pathogenicity.

Swimming and swarming motility

Ts-AgNPs significantly reduced the motility in *S. marcescens*. Swimming motility in *S. marcescens* was tested using sub-lethal concentrations of Ts-AgNPs. It was observed that 1/8 MIC Ts-AgNPs reduced the swimming motility of *S. marcescens,* while ¼ MIC- and ½ MIC-treated cells showed complete inhibition of swimming motility as compared to control (Fig. 6a2, a3, a4) and as compared to untreated control (Fig. 6a1). Ts-AgNPs showed reduced diameter of motility with increased Ts-AgNPs concentration. The diameter of swimming motility was 30 mm in 1/8th MIC, 10 mm in 1/4th MIC, and 0 mm in ½ MIC as compared to 38 mm in control cells (Fig. 6a5).

Similarly, even swarming motility of *S. marcescens* was also decreased drastically with Ts-AgNPs treatment in a dose-dependent manner (Fig. 6b1–b4). Control cells showed a diameter of 40 mm of swarming motility, while 1/8 MIC Ts-AgNPs-treated cells showed a diameter of 25 mm. Both ¼ MIC and ½ MIC Ts-AgNPs-treated cells showed complete inhibition of swarming motility in *S. marcescens* (Fig. 6b5).

Discussion

Multidrug-resistant bacteria have been causing severe infections that claim 13 lakh lives a year; of this, over 3.9 lakhs are just in South Asia alone. The ongoing COVID-19 pandemic has also led to an increase in the usage of antibiotics [40]. One of the major factors driving antibiotic resistance is the formation of biofilms by these bacteria [41–45]. The ability of bacteria to form biofilms is one of the main virulence factors that interfere with antibiotic activity and immune defence response mechanisms [43, 46, 47]. Among the biofilm-forming bacteria, *S. marcescens* showcases many virulence factors that are responsible for severe life-threatening infections [48]. It is a causative agent of wound infection, pneumonia, and urinary tract infection (UTI). The ability to form biofilms along with virulence factors plays a key role in providing this bacterium with resistance to antimicrobial drugs [49, 50]. As of now, no known drugs can mitigate *S. marcescens* biofilms, and it has attained a superbug status [51].

Antimicrobial treatment strategies have been bolstered by recently developed techniques, such as antibiotic cocktails, bacteriophage therapy, nanoparticles-based methods, natural compounds, and antimicrobial peptides [29, 52–56]. There has been significant research on the antibacterial properties of silver ions. In particular, some silver ions are highly efficient against both Gram-positive and Gram-negative bacteria. Such silver ions come from silver sulfadiazine and dissolved silver nitrate ($AgNO_3$). On the other hand, the highly reactive nature of silver ions drives down its antibacterial efficacy. With the rapid growth of nanotechnology in recent years, it is now possible to fabricate a variety of silver nanoparticles with increased antimicrobial efficacy due to their small size [57]. In the current study, Ts-AgNPs have been shown to be a potent antimicrobial agent for topical administration against multidrug-resistant bacteria in preclinical settings [58]. However, lack of colloidal stability, time-consuming synthesis procedures, cost, etc. pose major challenges in developing them for industrial and commercial applications [59]. Here, using tryptone as a stabilizing agent, we sought to mitigate the problems associated with colloidal stability, undesired toxicity, cost, time of their synthesis, and adverse effects on the ecosystem. Moreover, tryptone is known as a vital component in the nutrient media used for bacterial growth, and as such, it has no antibacterial effect. In the current study, using a combination of biochemical, microscopical, and cellular assays, highly efficacious antibacterial and antibiofilm activity of Ts-AgNPs in *S. marcescens* was demonstrated. As mentioned earlier, we took a facile synthetic approach for the synthesis of Ts-AgNPs and characterized them using an assortment of spectroscopic analyses and transmission electron microscopy [14]. First, the effect of these Ts-AgNPs on the planktonic growth of *S. marcescens* was carried out. Antibacterial activity of Ts-AgNPs was evidenced by lower MIC values and delay in the bacterial growth after the treatment with the nanoparticles (Fig. 1). Compared to most of the previous reports using different stabilizing/capping agents, the MIC values of Ts-AgNPs are substantially lower, indicating their superior efficacy [60–62]. It is documented earlier that the inhibitory effect of AgNPs on Gram-negative bacteria is more pronounced as compared to Gram-positive bacteria. One of the potential mechanisms that lead to this enhanced antibacterial activity in Gram-negative bacteria is the adsorption of the ionic form of silver (Ag +) by cytoplasmic membranes which ultimately leads to the destruction of the cell membrane, causing bacterial content leakage, and death [63]. Substantiating previous findings, the elevated levels of ROS by Ts-AgNPs observed in the current study, probably due to their interaction with the sulfur groups of some crucial proteins, facilitated bacterial death [64].

These results prompted us to investigate the impact of the Ts-AgNPs on the biofilm-forming ability of *S. marcescens*. It was observed that Ts-AgNPs efficiently inhibited biofilm formation in a concentration-dependent manner (Fig. 3A). Further, as demonstrated by a cell surface hydrophobicity assay, the Ts-AgNPs altered the hydrophobic properties of the bacterial cell wall, contributing, at least in part, to the inhibition of biofilm formation, demonstrating its prophylactic potential (Fig. 3B). On a therapeutic perspective, Ts-AgNPs effectively distorted preformed biofilms as evidenced via the interruption of EPS production (Fig. 4). These finding supports previous findings about the ability of AgNPs in inhibiting bacterial biofilms but with a considerably higher efficacy [65–73]. Concerning its mechanism of action, Ts-AgNPs likely diffuse through the EPS layer of the biofilm, and induced ROS production, prompting bacterial death, and thereby reducing EPS layer formation and dissolution of the biofilms. The antibiofilm ability of Ts-AgNPs to diffuse through the EPS layer has been reported earlier [74].

It is known that an important contributor to bacterial biofilm formation is their intercellular communication mechanism which is the quorum-sensing pathway. The quorum-sensing (QS) pathway, operated via chemical signals production, controls the bacterial response to extracellular signalling molecules and induces microbial virulence factors [75]. Ts-AgNPs demonstrated their ability to inhibit the production of QS-induced virulence factors. Specifically, as we observed, sub-MIC of the Ts-AgNPs efficiently inhibited the production of these virulence factors (such as urease, protease, lipase, prodigiosin pigment, and hemolysin) (Fig. 5) as reported earlier in other bacterial species [76]. Furthermore, Ts-AgNPs also significantly reduced the swimming and swarming motility in this bacterium indicating

their potential to inhibit both adhesion and dispersal stages of bacterial biofilms (Fig. 6), thereby attenuating the QS pathway and reducing bacterial biofilms [77].

Conclusion

The current study shows the effectiveness of tryptone-stabilized silver nanoparticles in interrupting bacterial growth and multiplication by altering the redox environment of the bacteria. Furthermore, Ts-AgNPs because of their small size diffused into the bacterial cells and inhibited biofilm formation by altering the cell surface hydrophobicity of this bacteria. It also effectively distorted pre-existing biofilms by inducing ROS production, and degrading eDNA, thereby distorting the EPS layer of biofilms, indicating their potential for both prevention and treatment of *S. marcescens*-associated diseases. Notably, Ts-AgNPs reduced various QS-induced virulence factors and their pathogenicity. Our study helps to understand the mechanistic details through which Ts-AgNPs interfere with bacterial persistence and antibiotic resistance, and might pave the way for developing Ts-AgNPs-based anti-biofilm therapeutics.

Supplementary Information The online version contains supplementary material available at https://doi.org/10.1007/s00775-022-01977-w.

Acknowledgements This work is supported by UM-DAE Centre for Excellence in Basic Sciences, Mumbai, India.

Data availability Data is available with the corresponding author and will be provided upon request.

Declarations

Conflict of interest The authors of this manuscript do not have any conflict of interest in publishing this work.

References

1. Lebeaux D, Ghigo JM, Beloin C (2014) Biofilm-related infections: bridging the gap between clinical management and fundamental aspects of recalcitrance toward antibiotics. Microbiol Mol Biol Rev 78:510–543
2. Roy R, Tiwari M, Donelli G, Tiwari V (2018) Strategies for combating bacterial biofilms: a focus on anti-biofilm agents and their mechanisms of action. Virulence 9:522–554
3. Jiang Y, Geng M (2020) Bai L (2020) Targeting biofilms therapy: current research strategies and development hurdles. Microorganisms 8:1222. https://doi.org/10.3390/microorganisms8081222
4. Kassinger SJ, Van Hoek ML (2020) Biofilm architecture: an emerging synthetic biology target. Synt Biotechnol 5:1–10
5. Brives C, Pourraz J (2020) Phage therapy as a potential solution in the fight against AMR: obstacles and possible futures. Palgrave Commun 6:100. https://doi.org/10.1057/s41599-020-0478-4
6. Rima M, Rima M, Fajloun Z, Sabatier J-M, Bechinger B, Naas T (2021) Antimicrobial peptides: a potent alternative to antibiotics. Antibiotics 10:1095. https://doi.org/10.3390/antibiotics10091095
7. Yang X, Ye W, Qi Y, Ying Y, Xia Z (2021) Overcoming multidrug resistance in bacteria through antibiotics delivery in surface-engineered nano-cargos: recent developments for future nano-antibiotics. Front Bioengin Biotechnol. https://doi.org/10.3389/fbioe.2021.696514
8. Ćirić AD, Petrović JD, Glamočlija JM, Smiljković MS, Nikolić MM, Stojković DS, Soković MD (2019) Natural Clinical and Laboratory Standards Institute (2003). Methods for dilution antimicrobial susceptibility tests for bacteria that grow aerobically; Approved standard-sixth edition. Wayne, Pa. USA: CLSI document M7-A6
9. Jeevanandam J, Barhoum A, Chan YS, Dufresne A, Danquah MK (2018) Review on nanoparticles and nanostructured materials: history, sources, toxicity and regulations. Beil J nanotechnol 9:1050–1074
10. Zia-ur-Rehman M, Naeem A, Khalid H, Rizwan M, Ali S, Azhar M (2018) Responses of plants to iron oxide nanoparticles. Nanomater. In plants, algae, and microorganisms. Academic Press, pp 221–238
11. Nirmala JG, Beck A, Mehta S, Lopus M (2019) Perturbation of tubulin structure by stellate gold nanoparticles retards MDA-MB-231 breast cancer cell viability. J Biol Inorg Chem 24(7):999–1007
12. Nirmala JG, Lopus M (2019) Tryptone-stabilized gold nanoparticles induce unipolar clustering of supernumerary centrosomes and G1 arrest in triple-negative breast cancer cells. Sci Rep 9(1):19126. https://doi.org/10.1038/s41598-019-55555-3
13. Mahaddalkar T, Mehta S, Cheriyamundath S, Muthurajan H, Lopus M (2017) Tryptone-stabilized gold nanoparticles target tubulin and inhibit cell viability by inducing an unusual form of cell cycle arrest. Exp Cell Res 360(2):163–170. https://doi.org/10.1016/j.yexcr.2017.09.002
14. Nirmala JG, Meher K, Lopus M (2022) Proteomic and metabolomic profiling combined with in vitro studies reveal the antiproliferative mechanism of silver nanoparticles in MDA-MB-231 breast carcinoma cells. J Mater Chem B. https://doi.org/10.1039/D1TB02760C
15. Mohanta YK, Singdevsachan SK, Parida UK, Panda SK, Mohanta TK, Bae H (2016) Green synthesis and antimicrobial activity of silver nanoparticles using wild medicinal mushroom *Ganoderma applanatum* (Pers.). IET Nanobiotechnol 10:184–189
16. Barillo DJ, Marx DE (2014) Silver in medicine: a brief history BC 335 to present. Burns 40:S3–S8. https://doi.org/10.1016/j.burns.2014.09.009
17. Jeremiah SS, Miyakawa K, Morita T, Yamaoka Y, Ryo A (2020) Potent antiviral effect of silver nanoparticles on SARS-CoV-2. Biochem Biophys Res Comm 533(1):195–200. https://doi.org/10.1016/j.bbrc.2020.09.018
18. Mittal AK, Chisti Y, Banerjee UC (2013) Synthesis of metallic nanoparticles using plant extracts. Biotechnol Adv 31:346–356
19. Kulkarni N, Muddapur U (2014) Biosynthesis of metal nanoparticles: a review. J Nanotechnol. https://doi.org/10.1155/2014/510246
20. Huang J, Lin L, Sun D, Chen H, Yang D, Li Q (2015) Bio-inspired synthesis of metal nanomaterials and applications. Chem Soc Rev 44:6330–6374
21. Gurunathan S, Han J, Park JH, Kim JH (2014) A green chemistry approach for synthesizing biocompatible gold nanoparticles. Nanoscale Res Lett 9:1–11
22. Mittal AK, Bhaumik J, Kumar S, Banerjee UC (2014) Biosynthesis of silver nanoparticles: elucidation of prospective

mechanism and therapeutic potential. J Colloid Interface Sci 415:39–47
23. Clinical and Laboratory Standards Institute (2003) Methods for dilution antimicrobial susceptibility tests for bacteria that grow aerobically; approved standard, 6th edn. CLSI document, Wayne, pp M7–M6
24. Bazargani MM, Jens R (2015) Anti-biofilm activity of essential oils and plant extracts against *Staphylococcus aureus* and *E. coli* biofilms. Food Control 61:156–164
25. Vishwakarma J, Vavilala SL (2020) Unraveling the anti-biofilm potential of green algal sulfated polysaccharides against *Salmonella enterica* and *Vibrio harveyii*. Appl Microbiol Biotechnol 104:6299–6314
26. Foucaud L, Wilson MR, Rown DM, Stone V (2007) Measurement of reactive species production by nanoparticles prepared in biologically relevant media. Toxicol Lett 1:1–9
27. Wang H, Joseph JA (1999) Quantifying cellular oxidative stress by dichlorofluorescein assay using microplate reader. Free Radic Biol Med 27:612–616
28. Shanks RM, Stella NA, Kalivoda EJ, Doe MR, O'Dee DM, Lathrop KL, Guo FL, Nau GJ (2007) A *Serratia marcescens* OxyR homolog mediates surface attachment and biofilm formation. J Bacteriol 189(20):7262–7272
29. Patel B, Mishra S, Indira Priyadarshini K, Sirisha VL (2021) Elucidating the anti-biofilm and anti-quorum sensing potential of selenocysteine against respiratory tract infections causing bacteria: in vitro and in silico studies. Biol Chem 402(7):769–783
30. Trentin DS, Giordani RB, Zimmer KR, da Silva AG, da Silva MV, Correia MT, Baumvol IJ, Macedo AJ (2011) Potential of medicinal plants from the Brazilian semi-arid region (Caatinga) against *Staphylococcus epidermidis* planktonic and biofilm lifestyles. J Ethnopharmacol 137:327–335
31. Ghodake V, Vishwakarma J, Vavilala SL, Patravale V (2020) Cefoperazone sodium liposomal formulation to mitigate *P. aeruginosa* biofilm in Cystic fibrosis infection: a QbD approach. Int J Pharmaceut 587:119696
32. Vishwakarma J, Waghela B, Falcao B, Vavilala SL (2021) Algal polysaccharide's potential to combat respiratory infections caused by *Klebsiella pneumoniae* and *Serratia marcescens* biofilms. Appl Biochem Biotechnol 194:671–693
33. Wang D, Jin Q, Xiang H, Wang W, Guo N, Zhang K (2011) Transcriptional and functional analysis of the effects of magnolol: inhibition of autolysis and biofilms in *Staphylococcus aureus*. PLoS One 6:e26833
34. Ansari MA, Khan HM, Khan AA, Cameotra SS, Pal R (2014) Antibiofilm efficacy of silver nanoparticles against biofilm of extended-spectrum β-lactamase isolates of *Escherichia coli* and *Klebsiella pneumoniae*. Appl Nanosci 4:859–868
35. Yanga D, Fana J, Caoa F, Denga Z, Pojmanb JA, Ji L (2019) Immobilization adjusted clock reaction in the urea–urease–H+ reaction system. RSC Adv 9:3514–3519
36. Salini R, Pandian SK (2015) Interference of quorum sensing in urinary pathogen *Serratia marcescens* by *Anethum graveolens*. FEMS Path Dis 73(2015):ftv038
37. Srinivasan R, Mohankumar R, Kannappan A, Karthick Raja V, Archunan G, Karutha Pandian S, Veera Ravi A (2017) Exploring the anti-quorum sensing and antibiofilm efficacy of phytol against *Serratia marcescens* associated acute pyelonephritis infection in Wistar rats. Cell Infect Microbiol 7:498
38. Eko Sukohidayat NH, Zarei M, Baharin BS, Manap MY (2018) Purification and characterization of lipase produced by *Leuconostoc mesenteroides Subsp. mesenteroides* ATCC 8293 using an aqueous two-phase system (ATPS) composed of triton X-100 and maltitol. Molecules 23(7):1800. https://doi.org/10.3390/molecules23071800
39. Khayyat AN, Hegazy WAH, Shaldam MA, Mosbah R, Almalki AJ, Ibrahim TS, Khayat MT, Khafagy E-S, Soliman WE, Abbas HA (2021) Xylitol inhibits growth and blocks virulence in *Serratia marcescens*. Microorganisms 9:1083. https://doi.org/10.3390/microorganisms9051083
40. Battling the superbugs: drug-resistant infections kill almost 1.3 m people a year. The Economist, Jan 22, 2022
41. Tacconelli E, Cataldo MA, Dancer SJ, De Angelis G, Falcone M, Frank U, Cookson B (2014) ESCMID guidelines for the management of the infection control measures to reduce transmission of multidrug-resistant Gram-negative bacteria in hospitalized patients. Clin Microbiol Infect 20:1–55. https://doi.org/10.1111/1469-0691.12427
42. Makharita RR, El-Kholy I, Hetta HF, Abdelaziz MH, Hagagy FI, Ahmed AA, Algammal AM (2020) Antibiogram and genetic characterization of carbapenem-resistant gram-negative pathogens incriminated in healthcare-associated infections. Infect Drug Resist 13:3991. https://doi.org/10.2147/IDR.S276975
43. Algammal AM, Hetta HF, Batiha GE, Hozzein WN, El Kazzaz WM, Hashem H, REl-Tarabili RM (2020) Virulence-determinants and antibiotic-resistance genes of MDR-*E. coli* isolated from secondary infections following FMD-outbreak in cattle. Sci Rep 10:1–13. https://doi.org/10.1038/s41598-020-75914-9
44. Farhan SM, Ibrahim RA, Mahran KM, Hetta HF, Abd El-Baky RM (2019) Antimicrobial resistance pattern and molecular genetic distribution of metallo-β-lactamases producing *Pseudomonas aeruginosa* isolated from hospitals in Minia. Egypt Infect Drug Resist 12:2125. https://doi.org/10.2147/IDR.S198373
45. El-Mokhtar MA, Hetta HF (2018) Ambulance vehicles as a source of multidrug-resistant infections: a multicenter study in Assiut City. Egypt Infect Drug Resist 11:587. https://doi.org/10.2147/IDR.S151783
46. El-Sayed Ahmed MAEG, Zhong L-L, Shen C, Yang Y, Doi Y, Tian G-B (2020) Colistin and its role in the Era of antibiotic resistance: an extended review (2000–2019). Emerg Microbes Infect 9:868–885
47. Abd El-Baky RM, Sandle T, John J, Abuo-Rahma GEDA, Hetta HF (2019) A novel mechanism of action of ketoconazole: inhibition of the NorA efflux pump system and biofilm formation in multidrug-resistant *Staphylococcus aureus*. Infect Drug Resist 12:1703. https://doi.org/10.2147/IDR.S201124
48. Khanna A, Khanna M, Aggarwal A (2013) *Serratia marcescens*- a rare opportunistic nosocomial pathogen and measures to limit its spread in hospitalized patients. J Clin Diag Res 7(2):243–246
49. Bakkiyaraj D, Sivasankar C, Pandian SK (2012) Inhibition of quorum sensing regulated biofilm formation in *Serratia marcescens* causing nosocomial infections. Bioorg Med Chem Lett 22(9):3089–3094. https://doi.org/10.1016/j.bmcl.2012.03.063
50. Ray C, Shenoy AT, Orihuela CJ, González-Juarbe N (2017) Killing of *Serratia marcescens* biofilms with chloramphenicol. Ann Clin Microbiol Antimicrob. https://doi.org/10.1186/s12941-017-0192-2
51. Baral B, Mozafari MR (2020) Strategic moves of "Superbugs" against available chemical scaffolds: signaling, regulation, and challenges. ACS Pharmacol Transl Sci 3(3):373–400. https://doi.org/10.1021/acsptsci.0c00005
52. Furfaro LL, Payne MS, Chang BJ (2020) Bacteriophage therapy: clinical trials and regulatory hurdles. Front Cell Infect Microbiol. https://doi.org/10.3389/fcimb.2018.00376
53. Mohanta YK, Biswas K, Jena SK, Hashem A, Abd AEF, Mohanta TK (2020) Anti-biofilm and antibacterial activities of silver nanoparticles synthesized by the reducing activity of phytoconstituents present in the Indian medicinal plants. Front Microbiol. https://doi.org/10.3389/fmicb.2020.01143

54. Al-Wrafy FA, Al-Gheethi AA, Ponnusamy SK, Noman EA, Fattah SA (2022) Nanoparticles approach to eradicate bacterial biofilm-related infections: a critical review. Chemosphere 288:132603
55. Mishra R, Panda AK, De Mandal S, Shakeel M, Bisht SS, Khan J (2020) Natural anti-biofilm agents: strategies to control biofilm-forming pathogens. Front Microbiol. https://doi.org/10.3389/fmicb.2020.566325
56. Di Somma A, Moretta A, Canè C, Cirillo A, Duilio A (2020) Antimicrobial and antibiofilm peptides. Biomolecules 10(4):652. https://doi.org/10.3390/biom10040652
57. Kędziora A, Speruda M, Krzyżewska E, Rybka J, Łukowiak A, Bugla-Płoskońska G (2018) Similarities and differences between silver ions and silver in nanoforms as antibacterial agents. Int J Mol Sci 19(2):444. https://doi.org/10.3390/ijms19020444
58. Mekkawy AI, El-Mokhtar MA, Nafady NA, Yousef N, Hamad MA, El-Shanawany SM, Elsabahy M (2017) In vitro and in vivo evaluation of biologically synthesized silver nanoparticles for topical applications: effect of surface coating and loading into hydrogels. Int J Nanomed 12:759. https://doi.org/10.2147/IJN.S124294
59. Mehta SM, Sequeira MP, Muthurajana H, D'Souza JS (2018) Rapid synthesis of gold and silver nanoparticles using tryptone as a reducing and capping agent. Appl Nanosci 8:759–769
60. Parvekar P, Palaskar J, Metgud S, Maria R, Dutta S (2020) The minimum inhibitory concentration (MIC) and minimum bactericidal concentration (MBC) of silver nanoparticles against *Staphylococcus aureus*. Biomater Investig Dent 7(1):105–109. https://doi.org/10.1080/26415275.2020.1796674
61. Loo YY, Rukayadi Y, Nor-Khaizura M-A-R, Kuan CH, Chieng BW, Nishibuchi M, Radu S (2018) In Vitro antimicrobial activity of green synthesized silver nanoparticles against selected gram-negative foodborne pathogens. Front Microbiol. https://doi.org/10.3389/fmicb.2018.01555
62. Wypij M, Czarnecka J, Świecimska M, Dahm H, Rai M, Golinska P (2018) Synthesis, characterization and evaluation of antimicrobial and cytotoxic activities of biogenic silver nanoparticles synthesized from *Streptomyces xinghaiensis* OF1 strain. World J Microbiol Biotechnol 34:23. https://doi.org/10.1007/s11274-017-2406-3
63. Bruna T, Maldonado-Bravo F, Jara P, Caro N (2021) Silver nanoparticles and their antibacterial applications. Int J Mol Sci 22(13):7202. https://doi.org/10.3390/ijms22137202
64. Martínez-Castañon GA, Nino-Martinez N, Martinez-Gutierrez F, Martinez-Mendoza JR, Ruiz F (2008) Synthesis and antibacterial activity of silver nanoparticles with different sizes. J nanopart res 10:1343–1348. https://doi.org/10.1007/s11051-008-9428-6
65. Hussain Z, Thu HE, Sohail M, Khan S (2019) Hybridization and functionalization with biological macromolecules synergistically improve biomedical efficacy of silver nanoparticles: reconceptualization of in-vitro, in-vivo and clinical studies. J Drug Deliv Sci Technol 54:101169. https://doi.org/10.1016/j.jddst.2019.101169
66. Davis SC, Li J, Gil J, Head C, Valdes J, Glinos GD, Pastar I (2019) Preclinical evaluation of a novel silver gelling fibre dressing on *Pseudomonas aeruginosa* in a porcine wound infection model. Wound Repair Regen 27:360–365. https://doi.org/10.1111/wrr.12718
67. Singh N, Rajwade J, Paknikar K (2019) Transcriptome analysis of silver nanoparticles treated with *Staphylococcus aureus* reveals potential targets for biofilm inhibition. Colloids Surf B 175:487–497
68. Habash MB, Goodyear MC, Park AJ, Surette MD, Vis EC, Harris RJ, Khursigara CM (2017) Potentiation of tobramycin by silver nanoparticles against *Pseudomonas aeruginosa* biofilms. Antimicrob Agents Chemother 61(11):e00415–e00417. https://doi.org/10.1128/AAC.00415-17
69. Thuptimdang P, Limpiyakorn T, Khan E (2017) Dependence of toxicity of silver nanoparticles on *Pseudomonas putida* biofilm structure. Chemosphere. https://doi.org/10.1016/j.chemosphere.2017.08.147
70. Hair BB, Conley ME, Wienclaw TM, Conley MJ, Berges BK (2018) Synergistic activity of silver nanoparticles and vancomycin against a spectrum of *Staphylococcus aureus* biofilm types. J Bacteriol Mycol 5:1089
71. Shafreen RB, Seema S, Ahamed AP, Thajuddin N, Alharbi S (2017) A Inhibitory effect of biosynthesized silver nanoparticles from the extract of *Nitzschia palea* against curli-mediated biofilm of *Escherichia coli*. Appl Biochem Biotechnol 183:1351–1361
72. Bala Subramaniyan S, Senthilnathan R, Arunachalam J, Anbazhagan V (2020) Revealing the significance of glycan binding property of Butea *monosperma* seed lectin for enhancing the antibiofilm activity of silver nanoparticles against uropathogenic *Escherichia coli*. Bioconjug Chem 31:139–148
73. Farooq U (2019) Rifampicin conjugated silver nanoparticles: a new arena for the development of antibiofilm potential against methicillin-resistant *Staphylococcus aureus* and *Klebsiella pneumoniae*. Int J Nanomed 14:3983
74. Foroohimanjili F, Mirzaie A, Hamdi SMM, Noorbazargan H, Hedayati Ch M, Dolatabadi A, Rezaie H, Bishak FM (2020) Antibacterial, antibiofilm, and anti-quorum sensing activities of photosynthesized silver nanoparticles fabricated from *Mespilus germanica* extract against multidrug resistance of *Klebsiella pneumoniae* clinical strains. J Basic Microbiol 60(3):216–230
75. Galloway WRJD, Hodgkinson JT, Bowden SD, Welch M, Spring DR (2011) Quorum sensing in gram-negative bacteria: small-molecule modulation of AHL and AI-2 quorum sensing pathways. Chem Rev 111(1):28–67
76. Singh BR, Singh BN, Singh A, Khan W, Naqvi AH, Singh HB (2015) Mycofabricated silver nanoparticles interrupt *Pseudomonas aeruginosa* quorum sensing systems. Sci Rep 5:13719
77. Hetta HF, Al-Kadmy IMS, Khazaal SS (2021) Antibiofilm and antivirulence potential of silver nanoparticles against multidrug-resistant *Acinetobacter baumannii*. Sci Rep 11:10751. https://doi.org/10.1038/s41598-021-90208-4